University of Stavanger

FACULTY OF SCIENCE AND TECHNOLOGY

BACHELOR THESIS

Study programme / specialization: Bachelor in Geosciences	The spring semester, 2022
	Open
Author: Ann Michelle van Achterberg	*Ann Michelle van Achterberg* (signature author)
Course coordinator: Alejandro Escalona Varela Supervisor: Carita Augustsson	
Thesis title: North-Sea basement and provenance of the Permian Rotliegend Group	
Credits (ECTS): 20	
Keywords: Pre-Devonian Basement North Sea Basement lithology Sediment transport direction Permian Rotliegend Group	Pages: 45 + appendix: 5 (pages) Stavanger, 15/05-2022 date/year

North-Sea basement and provenance of the Permian Rotliegend Group

By

Ann Michelle van Achterberg

BACHELOR THESIS

THE UNIVERSITY OF STAVANGER
MAY 2022

Acknowledgment

First of all I would like to thank my supervisor, Carita Augustsson, professor at the University of Stavanger, for excellent guidance and constructive feedback on my thesis.

I would also like to thank associate professor Dora Luz Marin Restrepo for nice discussions regarding volcanic rocks and for input on how to improve the basement lithology map in the North Sea.

In addition, I would also like to thank The Norwegian Petroleum Directorate (NPD) for providing core samples and thin sections for my study, and I am grateful for the opportunity to use their locals for core viewing.

I would also like to thank Lars Erik Berland for helpful discussions about interpretations of lithic fragments and sediment transport in the North Sea.

Finally, I would like to thank my family and friends for the support that I have received during my undergraduate study.

Table of Content

Abstract

Conglomerates and sandstones from the Permian Rotliegend Group contain clasts of Caledonian origin that suggests a basement source area and a sediment transport direction connected to the tectonic activity in Carboniferous and Permian time. The existing outline of the basement rocks in the Norwegian North Sea was incomplete, and therefore a new map of the basement lithologies was made based on core viewing and interpretations of crystalline thin sections from the Norwegian sector. Possible source areas and transport directions for Permian deposits were indicated based on point counting and core viewing of sandstones and conglomerates in the southern and western Norwegian North Sea with a specific focus on lithic fragments. The southern part of the Norwegian sector indicates phyllite and schist, whereas monzogranite, quartz-monzonite, monzodiorite, diorite, metasedimentary and mafic plutonic rocks, gneiss and andesite were identified in the western sector in the Norwegian North Sea. The cores and thin sections from the basement from the northern Norwegian sector show an abundance of dark gneiss. The crystalline clasts composed of monzogranite in conglomerates and sandstones in section 16 and 25 on the Utsira High suggests that the granitic area in sector 16 on the Utsira High acted as a source area to these Permian Rotliegend sedimentary rocks, resulting in a main sediment transport direction towards N-NW. The Rotliegend conglomerates also suggest that the underlying basement rock can act as a source rock due to fault activity. As a conclusion, the map of the basement lithologies and the interpretations of lithic fragments in Rotliegend sandstones and conglomerates are useful aids in reconstructing the post-Variscan sediment transport direction in the southern and western sectors of the Norwegian North Sea.

1. Introduction

The basement unit can be described as the deepest crystalline unit in the Earth's crust, and in the North Sea, the basement is made up of crystalline rocks of different lithologies from Precambrian to Silurian periods (Coward et al., 2003). The different lithologies in the basement reflect several tectonic events that have affected the North Sea, among them the Caledonian and the Variscan orogenies (Fossen et al., 2008B; Larsen et al., 2008).

The Permian Rotliegend Group in the North Sea seems to have been affected by syn-sedimentary tectonic activity (Leeder and Hardman, 1990). Paleozoic deposits and the Caledonian basement were uplifted and eroded during Late Carboniferous to Permian time, resulting in large amounts of detrital components that were transported into local basins (Fossen et al., 2008A; Larsen et al., 2008; Worsley & Nøttvedt, 2008). A theory is that the basement rocks may be source rocks to the sedimentary units of the Permian Rotliegend Group that were deposited in the present day North Sea at the time. Riber et al. (2015), Bassett (2003) and Slagstad et al. (2011) studied the lithology of the basement in the Norwegian sector of the North Sea. The variation of the crystalline basement rocks that is provided to this day is not complete, and a small study with focus on this variation could improve and update the understanding of this variation.

This study focuses on the basement rocks in the Norwegian sector of the North Sea, and the main objective of this thesis is to create a new and improved lithological map of the variation in crystalline rocks in the basement of the Norwegian North Sea based on core viewing and observations from crystalline thin sections. The study will also aim to cover the provenance of Rotliegend sandstones and conglomerates overlying the basement rock to understand the processes that have affected this unit.

2. Geologic setting

The North Sea has been affected by several tectonic events through history, especially during the Paleozoic (Coward et al., 2003).

2.1. The Caledonian Orogeny

The Caledonian mountain chain was formed from Late Silurian to Early Devonian and was a result of the collision between the two large paleocontinents Laurentia (the North American continent) and Baltica (Northern Europe and Russia; Glennie, 1990B; Gee et al., 2012). When these two large continents started to drift towards each other in south-east and north-west direction in the Ordovician, the initial stages of the closing of the Iapetus ocean, which was situated between the two continents, began (Glennie, 1990B; Gee et al., 2012). With time, a mountain chain was formed that stretched from the present day western Europe in the south

and up north to Svalbard (Coward, 1995; McKerrow et al. 2000). The collision between Laurentia and Baltica led to a new major continent called Laurussia (Glennie, 1990B).

In the initial stages of the collision, oceanic crust was subducted and island arcs were created, which both of the continents collided with eventually (Fossen, 2008; Fossen et al., 2008B). As the collision between the continents started, the Baltica continent was subducted and the Laurentia continent worked as a bulldozer, shoving nappes of different sizes in front of it for hundreds of kilometers onto the Baltica continent, which affected the continental margin of Baltica (Fossen, 2008; Fossen et al., 2008B).

During this complex geological situation in the Middle to Late Devonian, a lot of erosion took place, affecting the original rocks of both the continents which resulted in a change in the topography (Wiest et al., 2020). These processes, along with the weakening of the lateral forces that acted during the collision, resulted in the collapse of the Caledonian mountain chain, whereby the continents involved drifted apart and the crust got thinner (Fossen et al., 2008A; Worsley and Nøttvedt, 2008). The alpine landscapes in for example present day Norway were weathered and eroded, leading to large masses of detrital components that were transported to local basins (Fossen et al., 2008A; Worsley and Nøttvedt, 2008).

2.2. The Variscan (Hercynian) Orogeny

The Variscan mountain belt, also called the Hercynian mountain belt, formed from the Devonian to the end of the Carboniferous and stretched from present day United Kingdom and Central Europe in the west through Denmark and towards Poland in the east (Coward et al., 2003; Glennie, 1990B; Larsen et al., 2008). The large southern Gondwana plate and the northern Laurussian plate drifted northwards (Glennie, 1990B). However, Gondwana drifted faster than Laurussia, resulting in a collision between the two large continents (Glennie, 1990B). This major collision led to a new "supercontinent" called Pangaea and the Variscan mountain belt (Ziegler and Shell International Petroleum Company, 1982). The rocks from the Variscan mountain belt indicate both post-Caledonian structures created in the forming of the Variscan Orogeny in addition to old and reworked structures such as strike-slip faults originating from the forming of the Caledonian Orogeny (Glennie, 1990B).

2.3. Permian - The Rotliegend Group

The Permian period was dominated by hot and arid conditions, and an explanation for this may be the northwards drifting of Laurussia which was located closer to the Equator at the time (Glennie, 1990A). The Permian deposits from the Early and Mid-Permian in the North Sea is often referred to as Rotliegend material, and these sediments are associated with continental desert environments such as sand dunes in addition to seasonal rivers (Larsen et al., 2008).

Volcanic activity and intrusions affected the present day North Sea, especially during the Early Permian, together with both uplift and erosion of Paleozoic sediments and thermal subsidence (Larsen et al., 2008; Francis, 1987). Typical for deposits in the Lower Rotliegend (Early Permian) in the North Sea is that they were affected by faulting, often as reactivated faults from the basement (Leeder and Hardman, 1990).

During the faulting associated with the formation of the Variscan mountain belt, a large basin called the Northern Permian Basin (or Danish-Norwegian Basin) was formed in the present day southern North Sea area, which with time was filled with sediments of Caledonian origin in the Upper Rotliegend Subgroup (Mid-Permian deposits; Larsen et al., 2008; Glennie, 1990B).

2.4. The Utsira High

The Utsira High, which is a basement high, is located in the western part of the Norwegian North Sea (Osagiede et al. 2020). This high is associated with rifting activity, which affected the basement rocks in the area (Osagiede et al. 2020). The Utsira High is characterized by basement rocks encountered at a relatively shallow depth (Osagiede et al. 2020).

3. Methods

In this thesis, thirteen basement cores and eighteen corresponding and relevant crystalline thin sections from the Norwegian North Sea were looked at in addition to two available succeeding conglomerates and seven relevant thin sections of Rotliegend material (Tables 1, 2). The selection of the basement cores for this study was based on several aspects. Cores with available succeeding basal conglomerates were prioritized due to interest in the lithology of the clasts, and in addition, the goal was to make a map of the basement unit in the Norwegian North Sea, hence the attempt to include cores from different sections of the Norwegian sector. When discussed in the text, grain sizes, sorting, roundness and sphericity, and grain-grain contacts were provided according to Wentworth (1922), Longiaru (1987), Pettijohn et al. (1987) and Nichols (2009) respectively. For the classification of sandstones and statistical errors, the diagrams of McBride (1963) and Howarth (1998) were used respectively (Appendix 1). The thin sections were from the Norwegian Petroleum Directorate (NPD), and the information general information about them was collected from NPD (2021A). The sedimentary thin sections, in addition to thin sections 4-1, 4-2 and 13-2, were polished, but not stained, with one exception; thin section 9-1 was stained blue for porosity. The remaining basement thin sections were stained blue for porosity except for the thin sections from well 16/6-1 and they were not polished except for the two thin sections from depth 2058.7 m from well 16/6-1 and the thin sections from well 35/3-4.

3.1. Sedimentary samples - Point counting method

Point counting was performed for one conglomerate and four sandstones (Table 1) in two different ways for the thin section analysis with a polarizing microscope. The first point counting included all components (Appendix 3), whereas the other point counting focused on polycrystalline grains (Appendix 4). The goal was to count at least 300 grains to achieve good statistical results and to minimize uncertainties connected to the point counting, and this was achieved for thin sections 9-1 and 10-1, but exceptions were made for the conglomerate and the coarse sandstones due to larger grain sizes (Appendix 3). Several thin sections showed cracked minerals due to preparation, which was also a source of uncertainty when classifying the rocks. In the second point counting, the attempt was to include as many polycrystalline grains as possible to get a distribution of their origins (Appendices 2, 4), and everything else that was not polycrystalline was ignored.

Similar to the Gazzi-Dickinson method, grains of sand size ($\geq$ 63 μm) were counted as the mineral encountered in the cross-hair within the thin section with a limit between grains and matrix set to 63 μm (Dickinson, 1970). If quartz (and chert), feldspar or other minerals had inclusions of sizes > 63 μm, or other impurities, they were counted as lithic fragments in the thin section protocol (Appendix 3; Dickinson, 1970; Ingersoll, 1984). In this thesis, the lithoclasts were also classified further based on their origin in the second point counting (Appendix 4). Especially in this study, severely dissolved feldspar grains were counted as such if observed (Appendix 3). If twinning and cleavage directions were not visible, the feldspar grains were not classified further.

Table 1: The thin sections that were analyzed in the study.

| Well	Depth	Thin section	Lithology	Unit	Points counted
2/6-5	3231,00 m, 3234.00 m, 3237.00m, 3240.00 m, 3243.00 m, 3246.00m, 3249.00 m, 3252.00 m, 3253.00 m, 3254.00 m	3231,00 m, 3234.00 m, 3237.00 m, 3240.00 m, 3243.00 m, 3246.00 m, 3249.00 m, 3252.00 m, 3253.00 m, 3254.00 m	Phyllite	Pre-Devonian Basement	–
2/7-21S	5032.6 m, 4947.3 m	4-1 (x2), 4-2 (x2)	Rhyolite	Undefined Group, Devonian or older	–
2/7-31	4796.028 m, 4849.307 m	6-1, 6-7	Sandstone, conglomerate	Permian Rotliegend Group	68, 74
2/10-2	4151.1 m	7-1	Sandstone	Permian Rotliegend Group	264
8/3-1	3010 m	8/3-1.5-3010	Schist	Pre-Devonian Basement	–
9/4-5	5536.5 m	9-1	Sandstone	Permian Rotliegend Group	675
15/9-9	3032.2 m	10-1 (x2)	Sandstone	Permian Rotliegend Group	687
16/6-1	2058.7 m, 2060.50 m	16/6-1 #1 2058.7 m (x2), 16/6-1 core 1. 2060.50 m	Andesite, granodiorite	Pre-Devonian Basement	–
25/10-2R	3014.5 m	13-2	Conglomeratic clast	Permian Rotliegend Group (conglomerate)	–
35/3-4	4087.10 m, 4088.3 m	4087.10, 4088.3	Dark augengneiss, chlorite mica schist	Pre-Devonian Basement	–

3.2. Crystalline samples

The information about the cores were collected from NPD (2021B). Point counting was only performed for sedimentary samples. The crystalline cores and thin sections were described based on core viewing and microscopic observations of quality, quantity and other characteristics such as lithology and the color, shape and size of the crystals if possible, where the different crystals observed in all the basement cores are included in Table 3. The difference between fresh and weathered rock was also described if it was observed. If a conglomerate was succeeding the basement in the core, the lithology of the clasts and their abundance were described to gain more information about the processes affecting the basement. In addition, the clasts in the conglomerates were used to find out if the basement could be a source rock for the conglomerate or if other crystalline rocks were available for erosion in the region. During core viewing, fractures in the basement rocks were exposed to HCl acid (15 %) to check if they were filled with calcium carbonate.

The Norwegian sector of the North Sea is in this thesis divided into three zones considering the locations of the wells provided (Figure 1). Zone 1 includes the southern part of the Norwegian sector, whereas zone 2 is located in the western part around the Utsira High and zone 3 is in the north.

Table 2: The cores that were analyzed in the study.

Well	Depth	Unit	Zone
2/6-5	3252-3254.1 m	Pre-Devonian Basement	1
8/3-1	2968.4-2972 m, 3007-3015 m	Pre-Devonian Basement	1
16/1-4	1936-1941.7 m	Pre-Devonian Basement	2
16/1-12	1912-1938 m	Pre-Devonian Basement	2
16/1-17	1869-1987.45 m, 1987.45-1993.94 m	Triassic Hegre Group or Permian Rotliegend Group, Pre-Devonian Basement	2
16/3-2	2017.5-2019 m	Pre-Devonian Basement	2
16/4-1	2907-2909 m	Pre-Devonian Basement	2
16/5-1	1929-1942 m	Pre-Devonian Basement	2
16/6-1	2057-2060.5 m	Pre-Devonian Basement	2
25/10-2R	10424-10425 ft, 9888-1008 ft	Pre-Devonian Basement, Permian Rotliegend Group	2
25/11-1	7845-7858 ft, 8032-8065 ft	Pre-Devonian Basement	2
35/3-4	4087-4088.5 m	Pre-Devonian Basement	3
36/1-1	5210-5230 ft	Pre-Devonian Basement	3
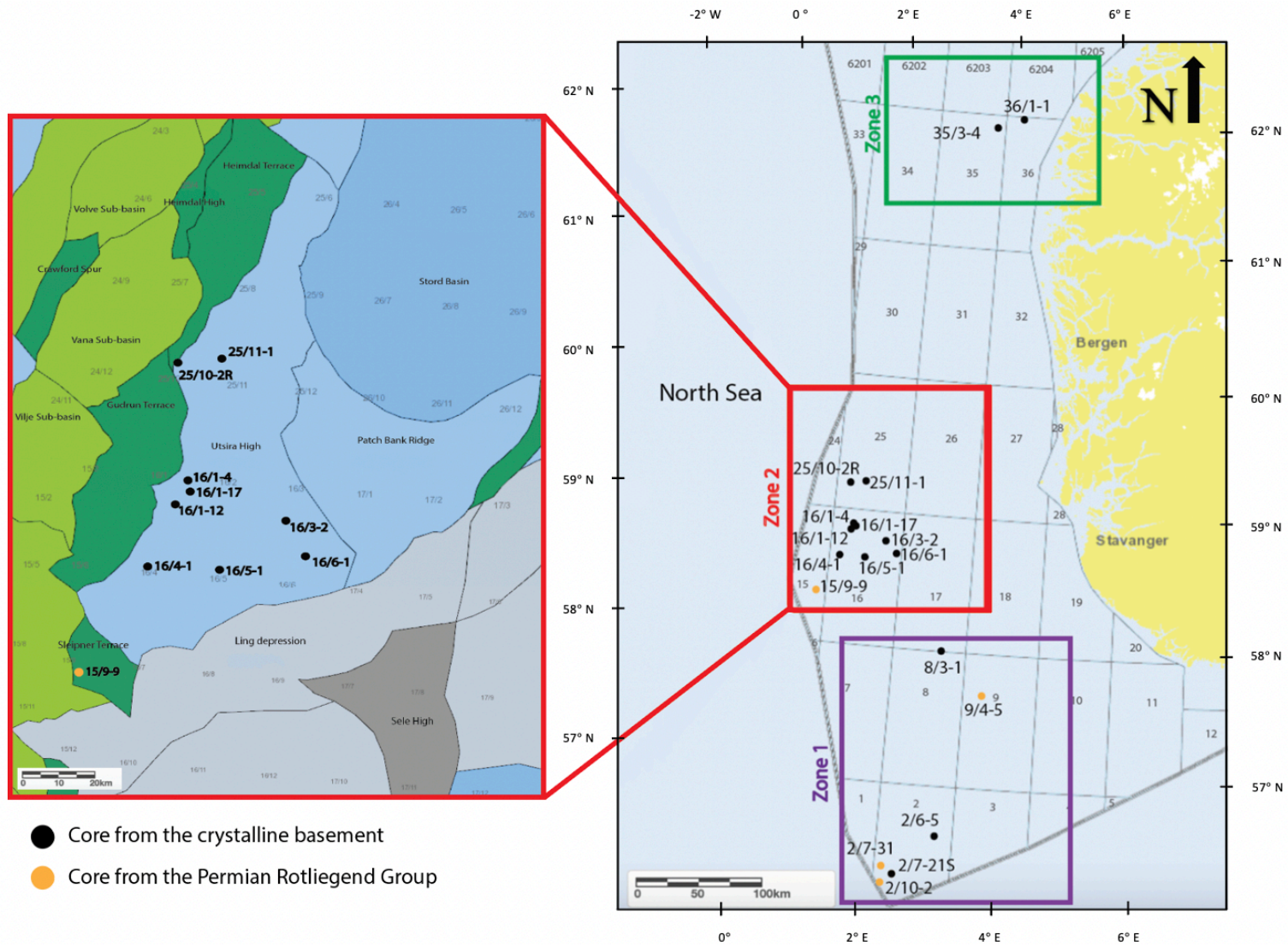
Figure 1: A map of the wells with samples of either cores or thin section from the crystalline basement or the Permian Rotliegend Group analyzed in this study. The map is from NPD (2022).

3.3. Map of the basement lithology

The map of the basement lithology was made based on analyzations from core viewing and crystalline thin sections of basement material. The basement lithologies were implemented the gravity anomaly map provided by Olesen et al. (2010) to compare the densities in the area with the lithologies from the basement in the attempt to interpret the boundaries of the basement lithologies. Based on a correlation between the densities and lithologies, boundaries could be drawn in a map, distributing the variety of the lithologies in the crystalline basement rock. Suggested boundaries for a lithology were set along a contour line illustrating a significant difference in density. The areas without samples were set as unknown, and wells with identified lithologies from other publications were included, but differentiated from interpretations from this study. Lithologies in sections that are assumed as local, such as the andesite in well 16/6-1, are not marked in the lithology map as their lithology, but as a part of the surrounding lithology.

4. Results

4.1. Cores from the basement – zone 1 (southern Norwegian North Sea)

The wells in the study that contain basement rocks in the southern part of the Norwegian sector in the North Sea are wells 2/6-5 and 8/3-1.

4.1.1. Well 2/6-5 – phyllite

The crystalline basement rock in well 2/6-5 is fractured and greyish green in color that has a metamorphic origin with a foliated texture and a shiny and wavy surface, indicating a medium metamorphic grade (Figure 2). The main minerals in this rock are quartz and alkalifeldspar, and minerals such as chlorite (hence the green color), muscovite and plagioclase are observed. There is also an unidentified black mineral present. It is difficult to measure the crystal sizes. The texture of the rock may resemble a schist in some sections, but based on the main texture and mineral content, this is a phyllite.

Thin sections 3253.00 m and 3254.00 m are classified as phyllites and they represent the fresh basement rock in the well. Both thin sections have a foliated texture with an alignment among the crystals, and the most abundant minerals are quartz, alkalifeldspar, muscovite and chlorite (Figure 2). Muscovite and chlorite are more abundant in thin section 3253.00 m than in thin section 3254.00 m. Plagioclase and opaque minerals occur in both thin sections.

The eight shallowest thin sections from well 2/6-5 (Table 1) show a weathered and fractured basement rock that is made up of clasts of different origins of mm sizes. There are two main types of clasts. One clast type resembles a mudrock and has a brownish red-colored fine groundmass with undulatory extinction and what looks like intrabasinal carbonate, which might have been foraminifers from the start, whereas the other type of clast is of metamorphic origin and consists of elongated crystals of undulatory quartz, plagioclase and muscovite that have sutured contacts and a direction among the crystals (Figure 2). Otherwise, opaque minerals appear in some of the clasts. The brownish red clasts decrease in size and amount with depth, while the metamorphic clasts increase in size and amount with depth. The metamorphic clasts are very similar to the fresh basement rock found in thin sections 3253.00 m and 3254.00 m.
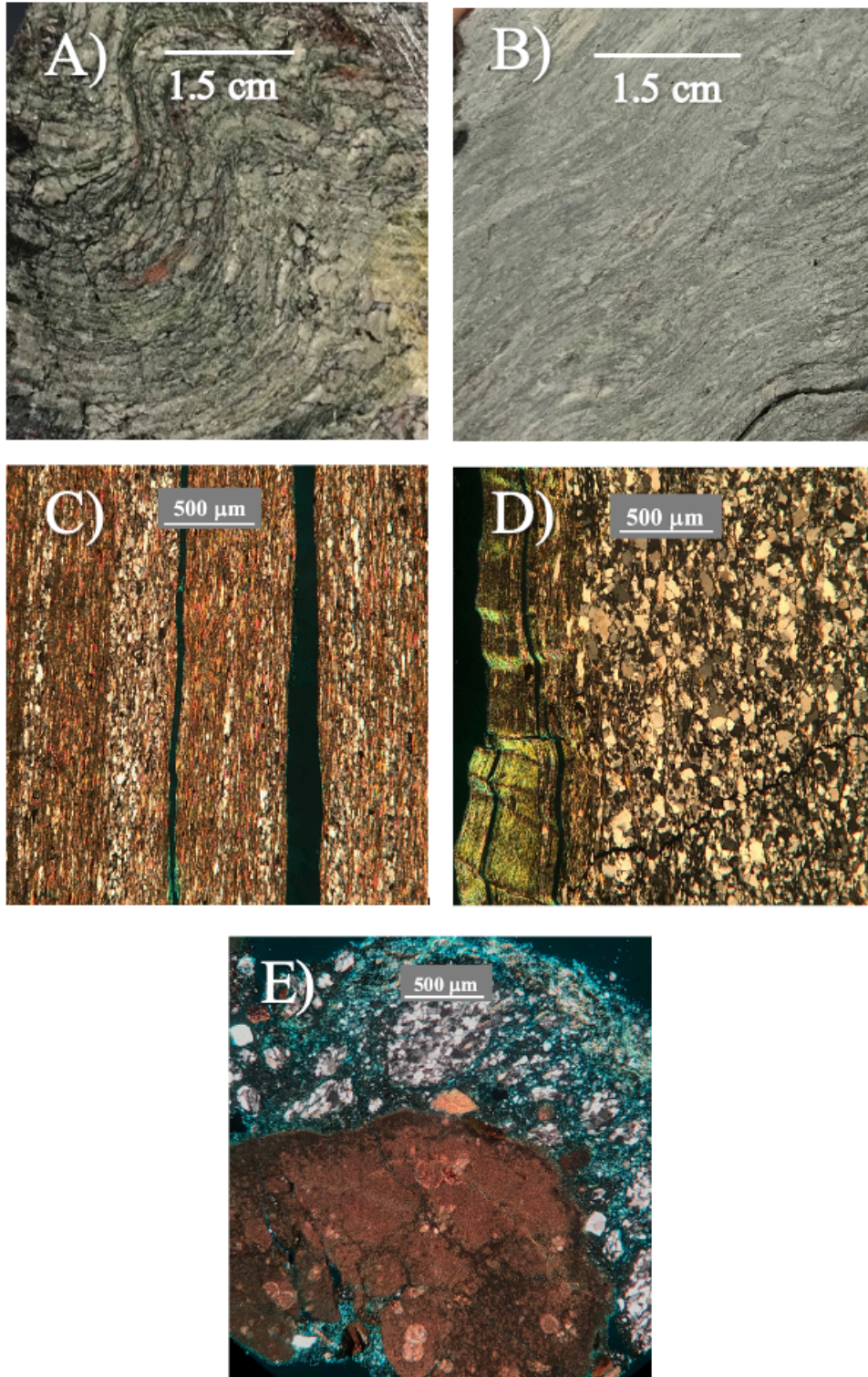
Figure 2: Phyllite from well 2/6-5. A) and B) are from a core, C) Thin section 3253.00 m, D) Thin section 3254.00 m, E) Thin section 3249.00 m illustrating the metamorphic and mudrock-looking clasts in the fractured basement.

4.1.2. Well 2/7-1S – rhyolite

Thin sections 4-1 and 4-2 from well 2/7-21S are volcanic rocks. Thin section 4-1 is a rhyolite, and thin section 4-2 is a brecciated rhyolite. They both have felsic compositions with voids and are rather dirty-looking with fine crystals of 40-210 μm in size. They consist mainly of undulatory quartz, alkalifeldspar and plagioclase. The feldspar minerals usually do not have twinning, but they have visible cleavage directions. Minor amounts of muscovite and opaque minerals are observed in addition to secondary carbonate cement in both thin sections.

4.1.3. Well 8/3-1 – schist

Core 4 in well 8/3-1 shows a grey and foliated metamorphic basement rock that consists of mostly quartz, plagioclase, biotite and alkalifeldspar (Figure 3). Other minerals such as chlorite, muscovite and other unknown black, oval and elongated minerals occur. There is alignment among the feldspar and quartz crystals, and the rock has light red and white-colored lenses that often resembles bonds that consist of alkalifeldspar and quartz respectively with widths of 1-3.5 mm. Fractures occur through the core and they are often filled with calcium carbonate. Based on the observations, this rock is a schist.

The crystalline basement rock in core 5 from the same well show similarities with the overlying rock, but with more varieties within it. This is a grey metamorphic rock with a shiny surface that is covered by clay minerals that are easily washed away (Figure 3). The rock has intrusions of red granite with crystal sizes of 1-3 mm in the deepest part of the core, but the intrusions are not observed in the shallower parts. The rock can be classified as a schist, and the main minerals are quartz, alkalifeldspar, plagioclase and biotite. Other minerals observed are chlorite, muscovite and pyrite.

The thin section from well 8/3-1 shows different types of textures. In one part, the thin section is plutonic with an abundance of quartz, alkalifeldspar and plagioclase, while another section is more deformed with an abundance of phyllosilicate minerals such as muscovite and biotite (Figure 3). Otherwise, chlorite, pyrite and other opaque minerals occur. There seems to be secondary carbonate cement in the rock. Based on the observations, this corresponds to the lithology in the deeper section from core 5 and can be classified as a chlorite mica schist with intrusion of granite.

Figure 3: Schist from well 8/3-1. A) Core 5, B) Core 4, C) Thin section from the well, illustrating both chlorite mica schist and granite.

4.2. Cores from the basement - zone 2 (western Norwegian North Sea)

4.2.1. Well 16/1-4 – diorite

The basement rock in well 16/1-4 consists of a dark, equigranular mafic plutonic rock with light-colored patches and intrusions of a light-red rock of felsic composition which is most likely syenite as alkalifeldspar is abundant and quartz is not present (Figure 4). The mafic rock is fractured and tectonically brecciated, and there is approximately the same amount of mafic and plutonic minerals in the rock. The light material consist of plagioclase and the mafic material is classified as hornblende based on the XRD analysis provided by Riber et al. (2015). Smaller amounts of alkalifeldspar and biotite occur, but quartz is not present. In the middle of the core, at depth 1939.7-1939.8 m, the lithology changes to a green, soft and smooth rock which may be a soapstone. Several deformed zones are observed in the rock in addition to veins with widths of 0.5-4 mm that are filled with secondary calcium carbonate. Based on the relatively light color and the composition of the rock, this may be a diorite.
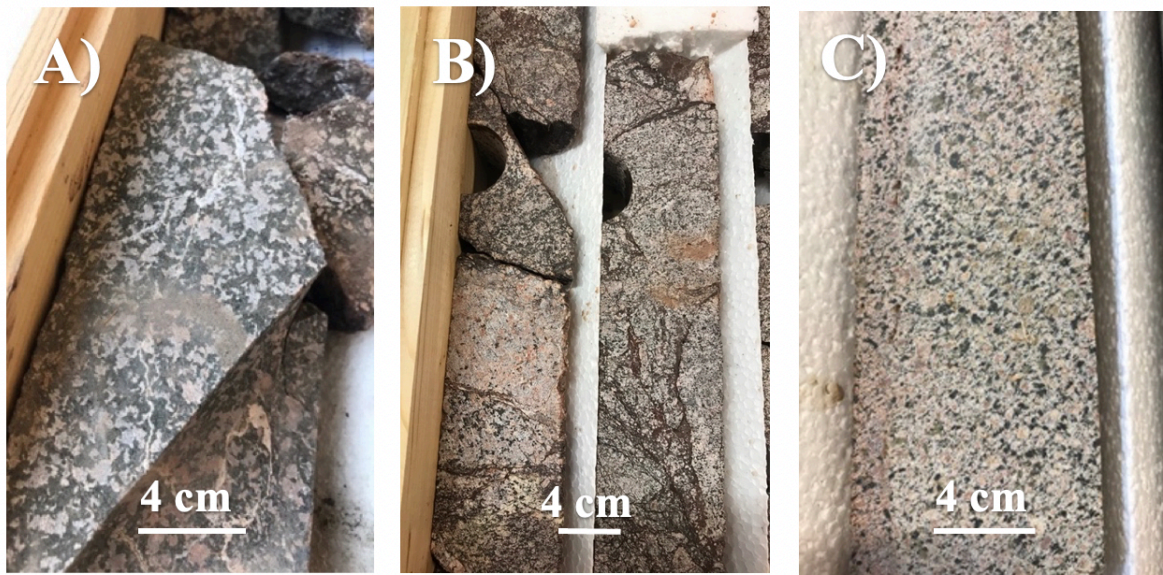

Figure 4: Cores from the western Norwegian North Sea. A) Diorite from well 16/1-4, B) Mafic plutonic rock with granite intrusion from well 16/1-17, C) Monzodiorite from well 16/1-12.

4.2.2. Well 16/1-12 – monzodiorite

Well 16/1-12 shows a fine-crystalline, weathered and mostly equigranular plutonic basement rock that is dominated by plagioclase (colorless), biotite (black) and alkalifeldspar (red) with mean crystal sizes of 1.5-4 mm in addition to smaller amounts of green, soft, elongated and rounded chlorite aggregates and light-brown clay aggregates (Figure 4). Some sections have coarser crystals of up to 9 mm, and some crystals have an internal color change with a dark red color in the outer part of the crystal and a gradually weaker color towards the core. Quartz crystals are not visible macroscopically. The rock can therefore be classified as a monzodiorite. There are color changes in the core in intervals of 20-30 cm where the rock changes from pink to greenish grey. In the greenish grey areas the fractures are often filled with calcium carbonate and they are often observed with a red color around them. The core provided includes 20-30 cm with overlying conglomerate with rounded clasts that are similar to the plutonic basement rock of sizes larger than 2 cm.

4.2.3. Well 16/1-17 – mafic plutonic rock

Well 16/1-17 contains a dark and severely weathered mafic plutonic basement rock which has intrusions of fresh and red granite with quartz, plagioclase and alkalifeldspar as the main minerals (Figure 4). The mafic plutonic rock consists of large amounts of amphibole, and there are fractures in the rock that are filled with calcium carbonate. Other than the amphibole minerals, it is difficult to identify the other minerals as the rock is weathered and fractured. Approximately 90 % of the core results in the mafic plutonic rock, and approximately 10 % results in the felsic granitic rock.

A section of medium-grained red sandstone with subrounded grains is observed within the basement core at depth 1990.23-1990.30 m with approximately 30 % of clasts that are 2-10 mm in size. The basement rock is overlain by 2.7 m of fine-grained sandstone, and the contact is relatively sharp with some small clasts of sizes 0.5-2 mm along the boundary. The color of the sandstone varies from brownish red to grey. Above this sandstone, a clast-supported conglomerate is present from depth 1869-1984.75 m with various clasts. The conglomerate is brownish red in color with some color variations. The rock is red above depth 1896.7 m, and it is mainly red below this depth but with lighter greyish green layers of 2-30 cm in thickness. The clasts in the conglomerate vary from pebble to cobble sizes. Most of the clasts in the

conglomerate are subrounded to rounded and of plutonic origin, although minor amounts of metamorphic and volcanic clasts occur, but they are not abundant. The plutonic clasts are present in the entire core and they are usually granitic and light red in color of different sizes. From the shallowest parts of the core and down to 1951 m in depth, cobbles occur, but they do not occur at deeper depths. They are usually light red-colored and granitic. The volcanic clasts do not appear deeper than 1935 m and they are subrounded and mafic, hence the dark color, and very fine-grained with light-colored phenocrysts of plagioclase within them. Some light grey metamorphic clasts appear as well, but only in the shallow parts. They have a clear direction among the elongated, subrounded and black unknown minerals in the clasts.

4.2.4. Wells 16/3-2, 16/4-1 and 16/5-1 – medium-crystalline monzogranites

There are several equigranular felsic plutonic basement rocks in the western Norwegian North Sea, and they are quite similar in composition. The main minerals in the plutonic basement rocks in wells 16/3-2, 16/4-1 and 16/5-1 are light-colored quartz and plagioclase in addition to red alkalifeldspar. Less abundant minerals are biotite and muscovite, in addition to an unknown red and squared mineral in well 16/3-2. The rocks are characterized as medium-crystalline monzogranites with crystal sizes of 0.5-2 mm, except from the core in well 16/3-2 which is coarse-crystalline with crystal sizes of 1-4 mm. The colors vary from dark to light red. The core from well 16/5-1 shows a fractured and weathered rock compared to the cores from well 16/3-2 and 16/4-1, which are fresh and not (or only slightly) fractured (Figure 5). The fractures are often filled with calcium carbonate in the deeper parts of the core in well 16/5-1, and around several of these fractures, the granite has lost its red color and turned greenish grey. Some areas in core 16/5-1 are dark red-colored due to hematite staining of clay minerals. The monzogranites are relatively homogeneous with one exception in the core from well 16/5-1 between 1937.5-1936.5 m, where there are less biotite crystals visible.

Figure 5: Monzogranites from wells A) 16/5-1, B) 16/3-2 and C) 16/4-1 located on the Utsira High.

The monzogranite in well 16/4-1 is succeeded by another rock of different lithology from depth 2908.3 m up to depth 2907 m with contact-metamorphic grade, and the contact between them is successive. The overlaying rock is a grey and greenish-yellow metasedimentary rock with an abundance of quartz and plagioclase with either light felsic layers of quartz and plagioclase or greenish yellow layers that most likely contain both chlorite and epidote with general thicknesses between 2 and 15 mm (Figure 6). Other less abundant minerals are biotite, alkalifeldspar and muscovite. In addition, there are unknown soft and red minerals and dark, elongated, rectangular and angular minerals that may be amphibole present with crystal sizes of 1-2 mm and 0.5-2 mm respectively. These crystals have their long axes in the same direction as the layers. Some sections in the rock are more deformed than others.
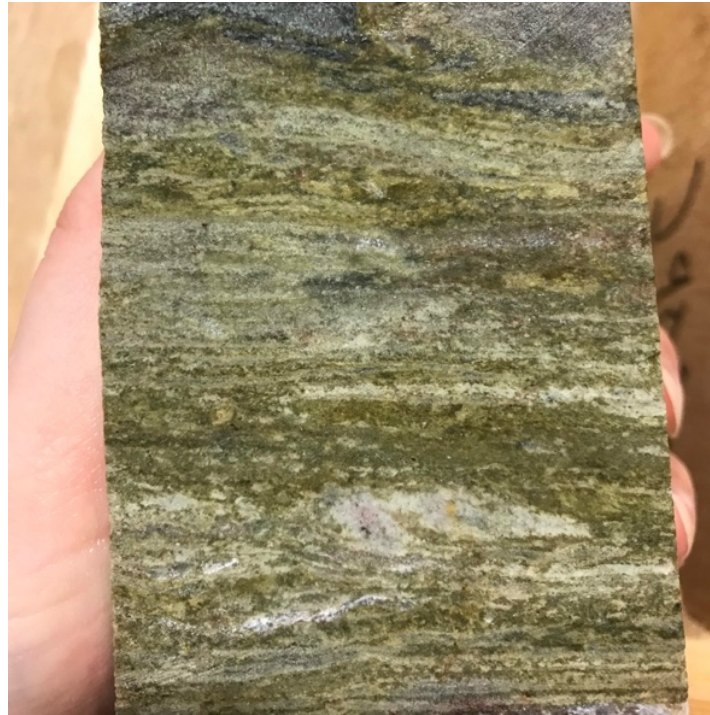
**Figure 6: Metasedimentary rock from well 16/4-1.**

4.2.5. Well 16/6-1 – andesite

The basement rock in well 16/6-1 is an intermediate and dark volcanic rock with a grey, relatively soft and very fine groundmass that most likely consist of plagioclase and may have been ash from the beginning (Figure 7). The volcanic rock contains 30-40 % soft, white or light grey plagioclase porphyroclasts which are blocky and rectangular in shape and range from 0.5-2 mm in size. Quartz is not visible macroscopically with an exception of a quartz vein that is present in the rock with a diameter of approximately 8 cm. Based on the porphyritic texture and the composition of the rock, this may be an andesite. From depth 2060.3 to 2060.5 m, the phenocrysts are absent, but the dark and fine groundmass is still present.

The two thin sections called 2058.7 m #1 from well 16/6-1 are quite similar and show a weathered volcanic rock composed of mostly plagioclase, both in the shape of small needles in the very fine groundmass and as phenocrysts of sizes ≤ 2 mm with albite twinning (Figure 7). There are also small amounts of biotite and alkalifeldspar with cross-hatched twinning present in addition to a small amount of quartz crystals (< 5 %) that usually appear as small phenocrysts with no sign of orientation. Small voids are observed. Based on the high amount of plagioclase and very small amount of quartz, this may be an andesite. Thin section 2060.5

m – core 1 on the other hand, which is collected from the deepest part of the core, show another lithology; a plutonic rock (Figure 7). The main minerals in this rock are plagioclase and quartz in a smaller amount. The plagioclase crystals either have polysynthetic twins or no twins at all. Other minerals that occur are biotite, chlorite and muscovite. This rock is not equigranular where one part of the thin section has large crystals compared to the rest of the crystals. Based on the mineral content, this may be a granodiorite.
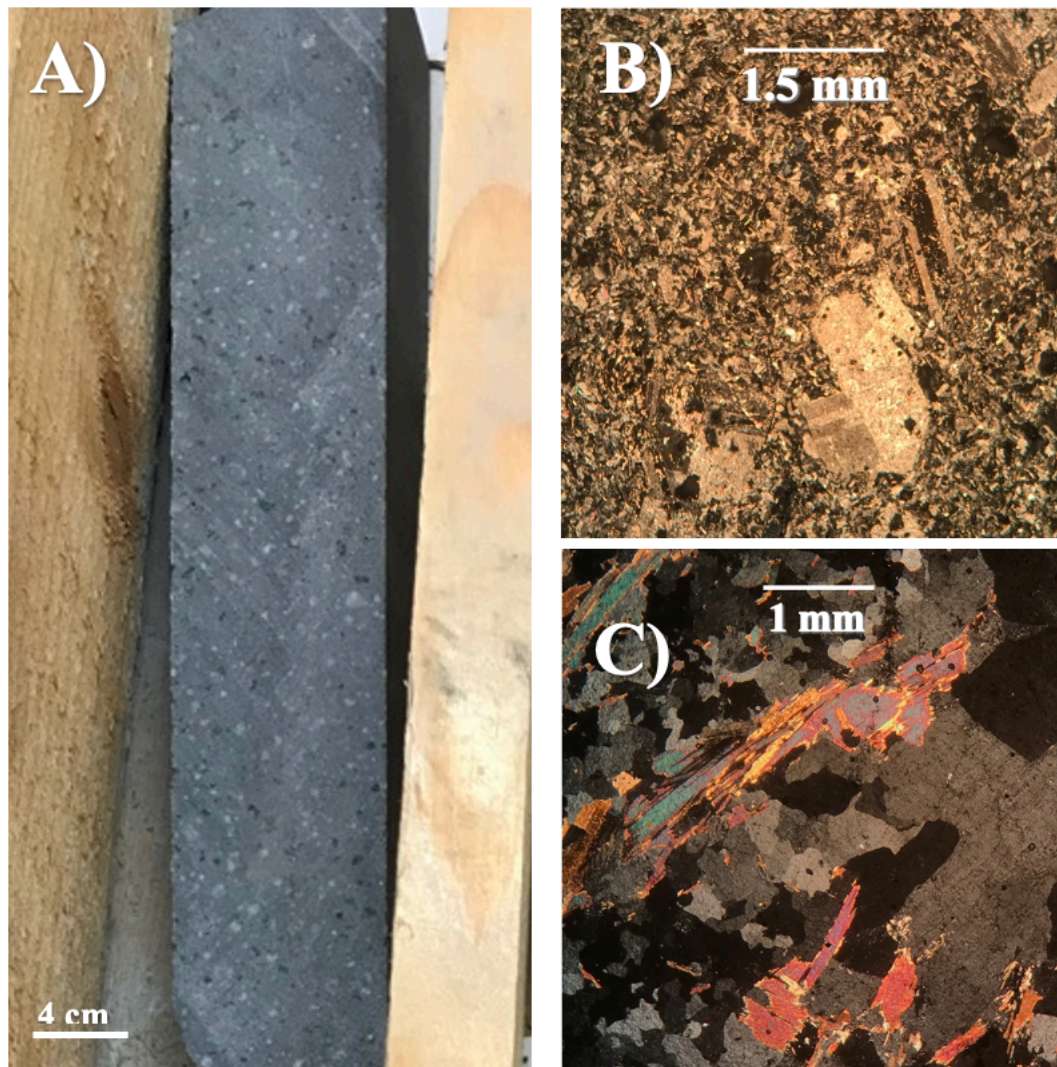
Figure 7: Samples from well 16/6-1. A) Core of an andesite, B) Thin section 2058.7 m #1 showing an andesite and C) Thin section 2060.5 m – core 1 showing a granodiorite.

4.2.6. Well 25/10-2R – quartz-monzonite

Well 25/10-2R has a fractured and greyish red-colored plutonic basement rock with a high content of plagioclase and alkalifeldspar in addition to smaller amounts of biotite (Figure 8).

Macroscopically quartz crystals are not observed in the rock with an exception of a small quartz vein of 2 mm in thickness in a rock fragment. The average crystal sizes are hard to identify in the fine-crystalline rock, and several fragments are covered in hematite. Based composition of the rock, this may be a fine-crystalline quartz-monzonite.

Figure 8: Quartz-monzonite from well 25/10-2R.

The Rotliegend conglomerate overlying the quartz-monzonite in well 25/10-2R contains large amounts of clasts similar to the underlying basement rock. The quartz-monzonite clasts are fine-crystalline, red-colored and often subrounded with medium sphericity, and some quartz crystals are visible macroscopically among the feldspar crystals. These clasts range from 4-37 mm in sizes and they appear abundantly in the deeper parts of the core and decreases in abundance upwards until depth 9888 ft, where they are absent. Along with the quartz-monzonite clasts, a lot of red and medium-crystalline granite clasts and some mafic volcanic clasts appear along most of the unit. Some of the mafic volcanic clasts contain plagioclase porphyroclasts.

Thin section 13-2 from well 25/10-2R is a clast from the conglomerate overlying the basement rock, and it shows a coarse-crystalline plutonic rock with an abundance of plagioclase and smaller amounts of undulatory quartz and alkalifeldspar, brown biotite, muscovite, opaque minerals and chlorite. The plagioclase crystals usually have polysynthetic

twins, and the alkalifeldspar crystals show cross-hatched twins. Based on the texture, this is most likely a monzogranite clast in the conglomerate.

4.2.7. Well 25/11-1 – light gneiss

The basement rock in core 14 in well 25/11-1 is a fresh and light grey-colored gneiss that mainly consists of quartz (Figure 9). Plagioclase and quartz occur in the light-colored bonds, and additional minerals are muscovite, chlorite and biotite. At depth 8032-8065 ft, the basement rock is fractured, and a red conglomerate with clasts resembling the basement rock is surrounding the fractured areas. The gneiss is also fractured from depth 7845-7858 ft and up to the end of core 14. Core 13 shows a weathered, slightly deformed and reddish brown rock that resembles a schist.
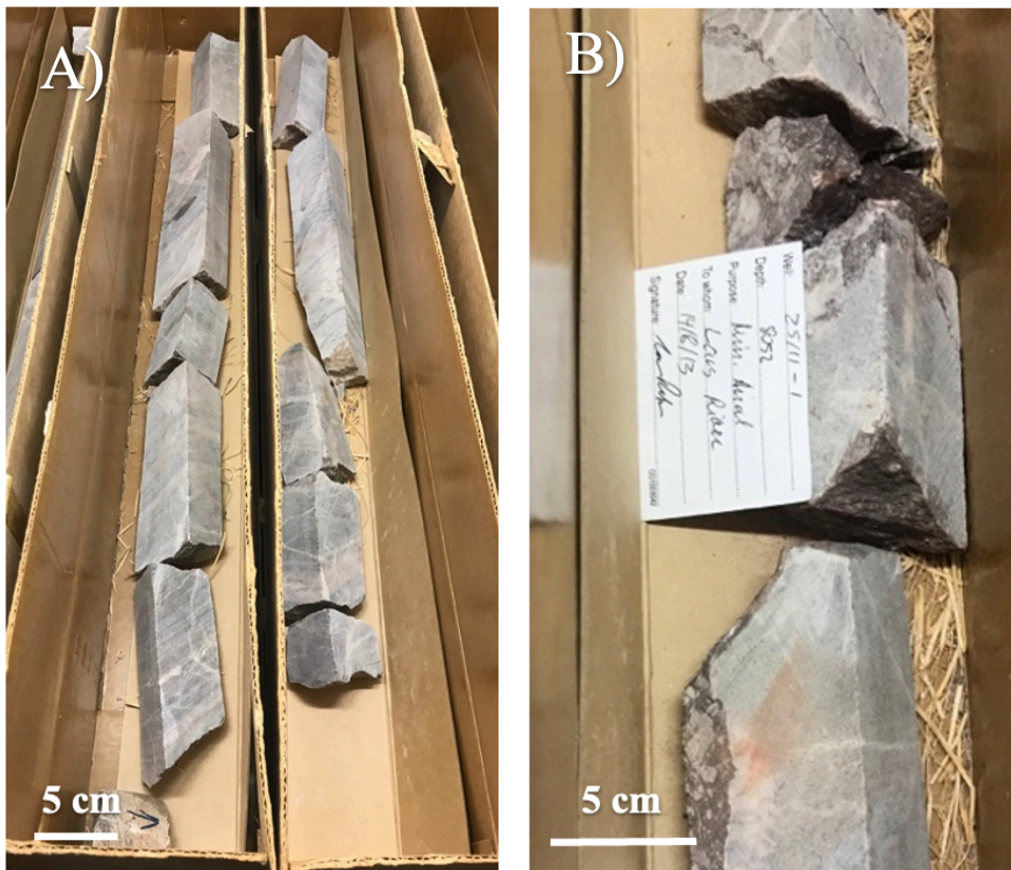

**Figure 9: A) Light gneiss and B) Light gneiss with conglomerate
surrounding the crystalline rock in core 14 in well 25/11-1.**

4.3. Cores from the basement - zone 3 (northern Norwegian North Sea)

4.3.1. Wells 35/3-4 and 36/1-1 –dark augengneiss, dark gneiss and chlorite mica schist

Wells 35/3-4 and 36/1-1 in the northern zone of the Norwegian North Sea have dark-grey crystalline and metamorphic basement rocks with quartz as the most abundant mineral (Figure 10). The second most abundant minerals are plagioclase and alkalifeldspar. The dark color of the rocks are results of the biotite content, and for well 35/3-4, amphibole is present as well. In addition, small amounts of muscovite (colorless), chlorite, pyrite (golden color) and some unknown, brown and rounded minerals occur in both wells. Biotite often appear as thin sheets in the same direction as the bonds in both of the rocks, and the pyrite crystals are elongated and rectangular with the long axis in the same direction as the bonds. Well 35/3-4 contains bonds that range from 0.25-0.4 cm in thickness that are either red-colored (alkalifeldspar and quartz) or white-colored (plagioclase and quartz) in addition to an abundance of augen of alkalifeldspar (0.9-2.5 cm). Based on composition and structure, the basement rock in well 35/3-4 is a dark augengneiss. Well 36/1-1 on the other hand has oval and elongated quartz porphyroblasts (0.6-2 cm) in a preferred direction. Based on the bonds in the rock, the basement rock in well 36/1-1 can be classified as a dark gneiss with quartz porphyroblasts.

The gneiss in well 35/3-4 is fractured, and a shiny dark and light-green surface appear in the fractures, confirming the content of biotite and chlorite. The deepest part of well 35/3-4, from depth 4088.3 m and deeper, has another lithology. This section is classified as a chlorite mica schist, which indicates larger amounts of chlorite, hence the green color, in addition to muscovite, biotite, amphibole and pyrite in the wavy texture (Figure 10). A similar composition is found in thick bonds that contain mostly mafic components in the gneiss in well 36/1-1 of 1.7-3.9 cm in thickness with crystal sizes of 0.5-3 mm, but the bonds are straight. In addition, the gneiss in well 36/1-1 has several fractures with widths of 1-3 mm that are filled with calcium carbonate.
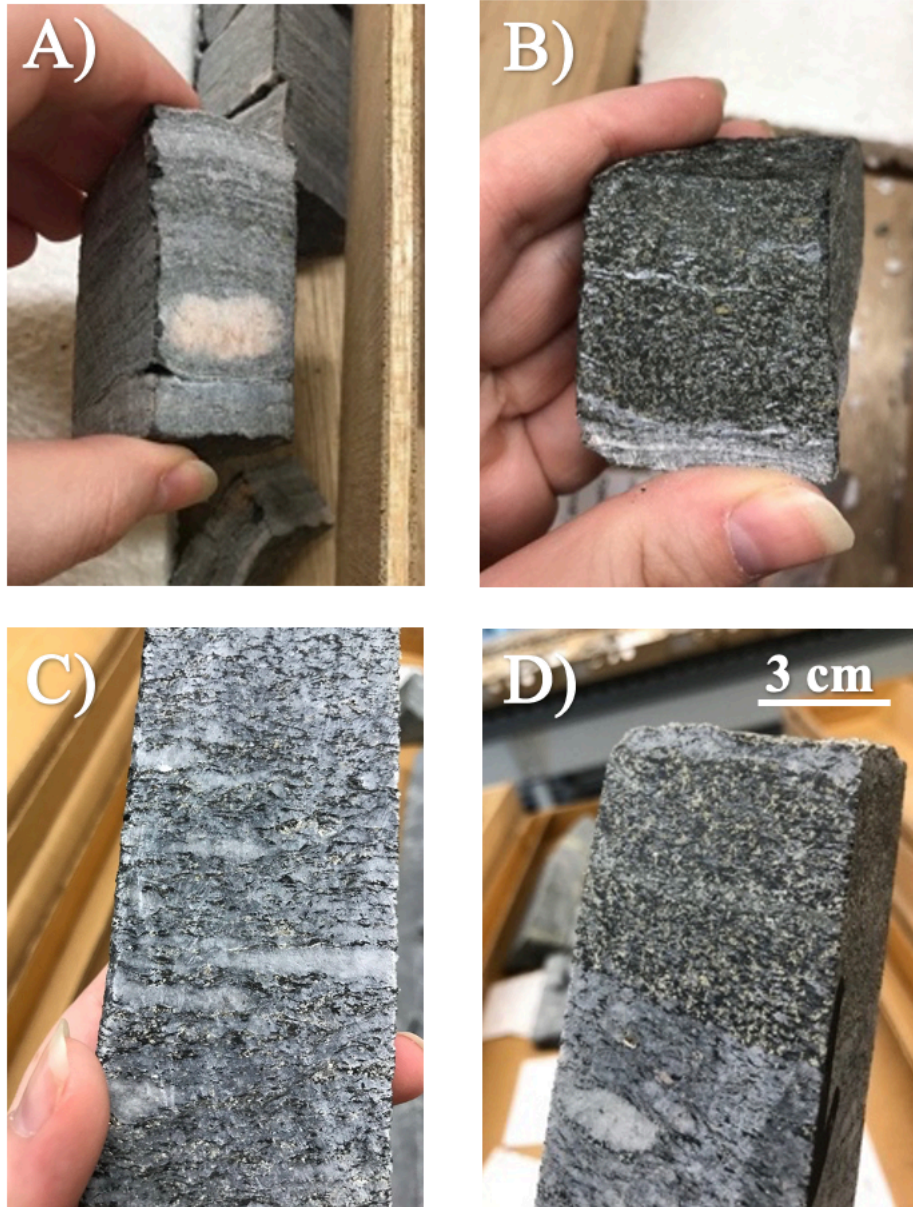
Figure 10: Basement rocks from wells 35/3-4 and 36/1-1. A) Augengneiss from well 35/3-4, B) Chlorite mica schist from well 35/3-4, C) Augengneiss from well 36/1-1, D) Bonds of mafic composition in well 36/1-1 similar to the chlorite mica schist in well 35/3-4.

The two thin sections from well 35/3-4 are both of metamorphic origin, but they are slightly different. Thin section 4087.10 shows a gneiss with bonds of mostly quartz and plagioclase with muscovite in the same direction as the bonds. A small amount of opaque minerals is also present. Thin section 4088.3 on the other hand is a schist with an abundance of quartz, chlorite, biotite, plagioclase and muscovite. Pyrite and an unknown, rounded and colorless mineral with high relief are also observed. The abundance of chlorite and mica minerals makes thin section 4088.3 a chlorite mica schist.

Table 3: An overview of the mineral content observed macroscopically in the basement rocks in the Norwegian North Sea.

Well	Lithology (core number)	Main minerals	Other minerals	Unknown minerals (not abundant)
2/6-5	Phyllite	Qrtz > A-fspr	Chl – Mus – Plg	Black mineral
8/3-1	Schist (4)	Qrtz – Plg > Bio - A-fspr	Chl > Mus	Black mineral
	Schist (5)	Qrtz – A-fspr > Plg – Bio	Chl > Mus > Pyr	
16/1-4	Diorite	Plg – Hbl	A-fspr – Bio	
16/1-12	Monzodiorite	Plg > Bio > A-fspr	Chl	
16/1-17	Mafic plutonic rock	Amph		
16/3-2	Coarse-crystalline monzogranite	Qrtz – Plg > A-fspr	Bio > Mus	Red mineral
16/4-1	Medium-crystalline monzogranite	Qrtz – Plg > A-fspr	Bio > Mus	
	Metasedimentary rock	Qrtz – Plg	Epid – Chl > A-fspr – Bio – Mus > Amph	Red mineral
16/5-1	Medium-crystalline monzogranite	Qrtz – Plg > A-fspr	Bio > Mus	
16/6-1	Andesite	Plg	A-fspr	
	Granodiorite	Plg		
25/10-2R	Fine-crystalline quartz-monzonite	Plg > A-fspr	Bio > Qrtz	
25/11-1	Light gneiss	Qrtz	Plg > Mus – Bio > Chl	
35/3-4	Dark augengneiss	Qrtz >> A-fspr – Plg – Bio – Amph	Chl > Mus > Pyr	Brown mineral
	Chlorite mica schist	Chl – Mus – Bio – Qrtz – Plg	Pyr	
36/1-1	Dark gneiss with quartz porphyroblasts	Qrtz >> A-fspr – Plg – Bio	Mus > Pyr	Brown mineral

A-fspr = Alkalifeldspar, Apmh = Amphibole, Bio = Biotite, Chl = chlorite, Epid = Epidote, Hbl = Hornblende, Mus = Muscovite, Plg = Plagioclase, Pyr = Pyrite, Qrtz = Quartz

4.4. Map of basement lithologies in the Norwegian North Sea

The classified lithologies from the basement rocks analyzed in both the cores and thin sections are correlated with densities of the surface in the corresponding areas from Figure 11. There are relatively low densities in the southern section where phyllite and schist are the suggested lithologies. There are also low densities in areas corresponding to the gneisses from wells 35/3-4 and 36/1-1 in the northern region. In the western part of Figure 11, an area with high density is classified as granite as the location of the basement granites correlate with this interval. Plagioclase-rich plutonic rocks are surrounding this granitic area.

The variation of the crystalline basement rocks is illustrated in Figure 12 for all the zones, where zone 1, which corresponds to the southern Norwegian sector, indicate phyllite and schist as basement rocks, whereas the western part of the Norwegian North Sea, zone 2, has several different basement lithologies with granite and plagioclase-rich plutonic rocks as the most abundant lithologies. Zone 3, the northern sector, show an abundance of gneiss. Lithologies from other studies are also implemented in the map and contribute to a better visualization of the suggested variations in the basement.
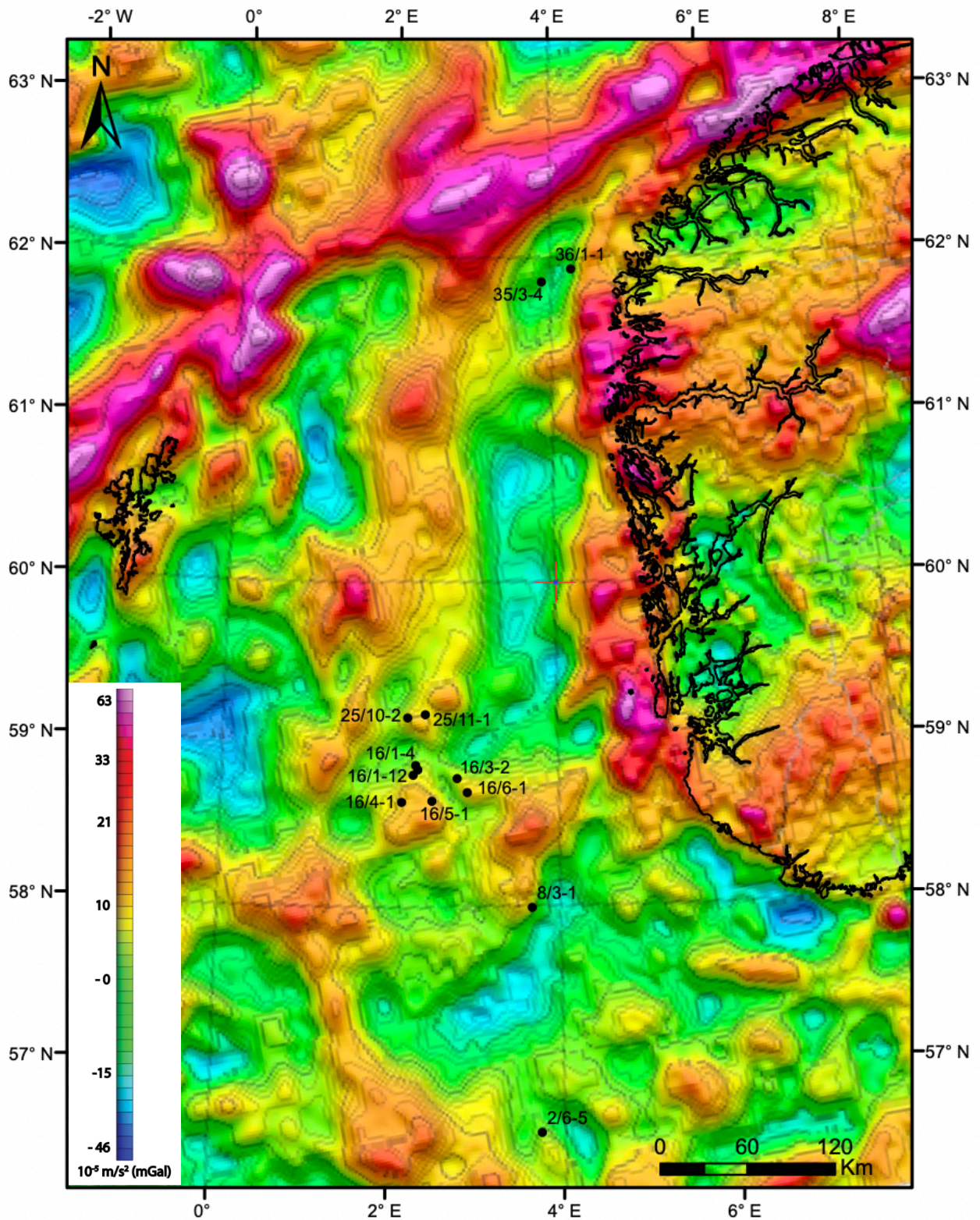
Figure 11: Cores with basement rocks plotted into the gravity anomaly map from Olesen et al. (2010). This map is made by Dora Luz Marin Restrepo.
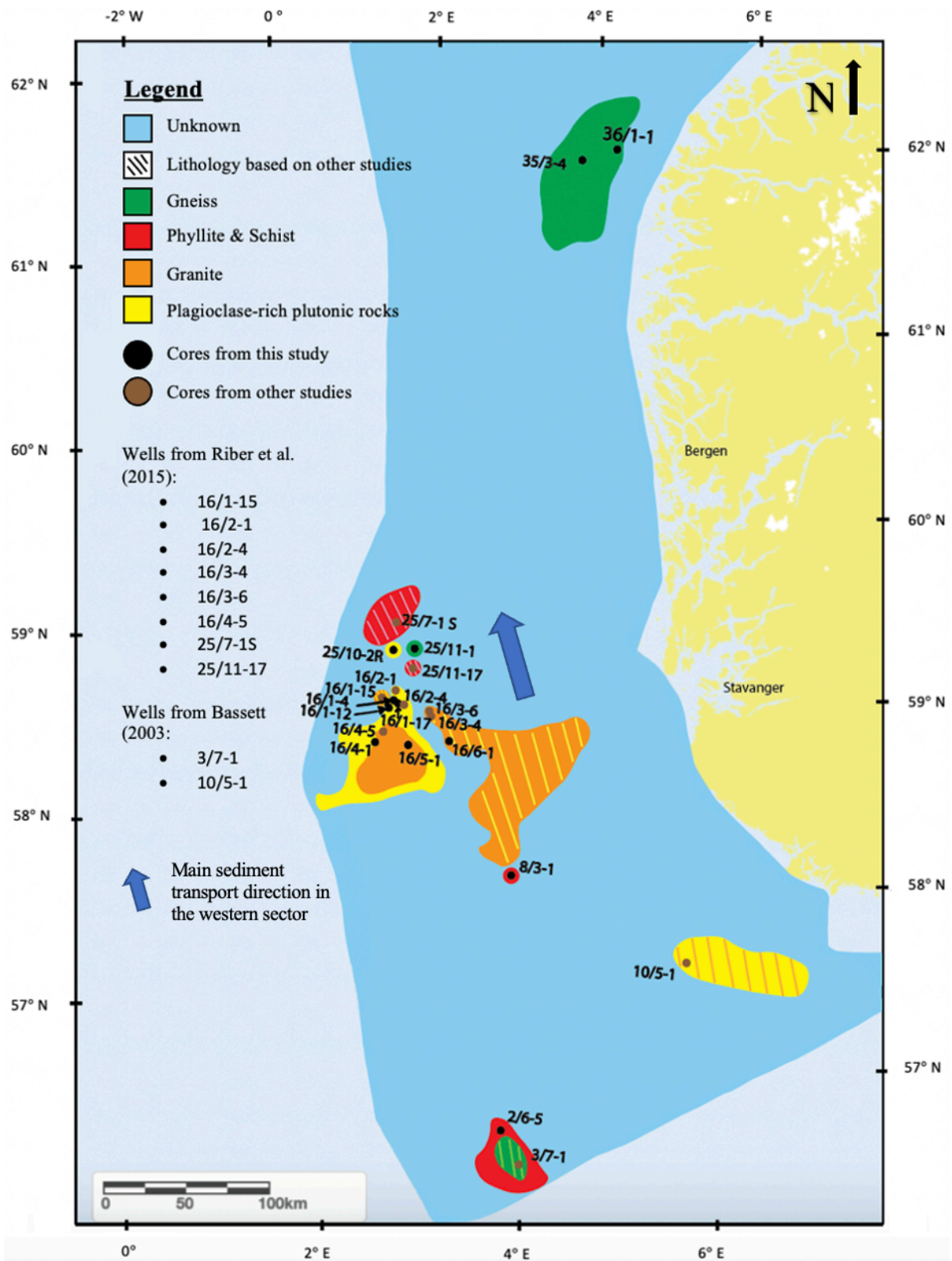
Figure 12: A lithology map of the basement in the Norwegian North Sea which also illustrates the main sediment transport direction in the western sector. The map is modified from NPD (2022).

4.5.Petrography of conglomerate and sandstone

The conglomerate in thin section 6-7 is polymodal with a coarse matrix and three different grain sizes with intervals of 0.5-1.0 mm (coarse matrix), 1.6-4.0 mm and 6.7-10.8 mm. The conglomerate has very poor sorting, subrounded grains with medium sphericity and an abundance of plane contacts, although some concave-convex contacts and point contacts occur.

Quartz is the most abundant mineral in the conglomerate with 55 %. The monocrystalline quartz grains are usually a part of the coarse matrix with grain sizes of 500-870 μm with some exceptions. Undulatory quartz is more abundant than non-undulatory quartz and the monocrystalline quartz grains are often subrounded to rounded, elongated and oval with medium to high sphericity. They also have a tendency to have inclusions in them, which distinguishes them from feldspar grains.

Polycrystalline quartz grains are abundant in this sedimentary sample with approximately 19 % with the same roundness, sphericity and shapes as the monocrystalline quartz grains. These grains are larger than the monocrystalline grains and range from 0.95-7.0 mm in size. The polycrystalline quartz grains seem to have two different origins, where 65 % are of metamorphic origin and 35 % are of plutonic origin (Appendices 2, 4). The grains with metamorphic origin usually have 2 indented crystals or more with sutured contacts and a clear direction among the elongated and undulatory indented quartz crystals. The plutonic grains do not have a direction and they often have a mosaic structure with straight contacts.

Chert grains are present, but not abundant, with 3 % in the conglomerate with grain sizes of 500-760 μm. Most of the grains are coarse-crystalline, but fine-crystalline chert appear as well. The chert grains are dirty-looking with black dots and they are usually oval, subrounded to rounded and elongated with medium sphericity.

Feldspar is the second most abundant mineral in the conglomerate with 5 % and a mean grain size of 540 μm. They usually do not have twinning or cleavage directions visible, although plagioclase with polysynthetic twins is observed. They are often subrounded and elongated with medium sphericity and rectangular shapes. They may appear as undulatory and slightly dissolved in the edges, but not abundantly.

Lithic fragments result in 12 % of the grains in the conglomerate and they have a wide grain size interval of 0.93-10.8 mm. Among the lithic fragments, there are 80 % metamorphic and 20 % plutonic lithoclasts (Appendices 2, 4). The metamorphic lithoclasts are mainly composed of quartz and feldspar, but may also include muscovite, biotite and opaque minerals as well, and they have sutured contacts between the indented and elongated crystals. Most importantly, they have a characteristic direction within the indented crystals, and the quartz crystals often have undulatory extinction. The muscovite crystals are in the same direction as the other crystals in the fragment. The plutonic fragments have similar composition as the metamorphic ones, but they do not have a direction among the crystals in the fragment. They usually have a mosaic structure with straight contacts between the crystals. The lithic fragments in the conglomerate are often rounded with medium to high sphericity and they are the largest grains present in the thin section.

The accessory minerals in thin section 6-7 are muscovite, biotite and opaque minerals. Dickite and feldspar cement in addition to quartz matrix also occur in the sample.

The conglomerate is not very porous with 7 % in form of intergranular pores, and it is not very cemented either with 7 %, where illite and quartz cement are most abundant. Phyllosilicate matrix occur, but not frequently.

The sandstones analyzed in this study are from sector 2, 9 and 15 in the Norwegian North Sea, but despite the different locations, they have several similarities. Thin sections 9-1 and 10-1 are classified as medium-grained sandstones with a general grain size interval of 275-290 μm. They are well sorted with grains that are subrounded with medium sphericity and with an abundance of plane contacts, although some concave-convex contacts are observed. Thin sections 6-1 and 7-1 has the same characteristics as the other two sandstones with the exception that they are coarser with mean grain sizes of 940 μm and 750 μm respectively. Thin section 7-1 is moderately sorted and classified as a coarse-grained sandstone, while thin section 6-1 is poorly sorted and classified as a conglomeratic sandstone based on grain size. The sandstones in thin sections 6-1 and 7-1 has up to 4 grains that are above 2 mm in size, and thin section 6-1 contains a pebble of size 6.1 mm. Based on the composition of the sandstones, thin sections 7-1 and 9-1 are classified as arkoses, whereas thin section 10-1 is classified as a subarkose and thin section 6-1 is classified as either a sub-litharenite or a lithic subarkose. The sandstones in thin sections 9-1 and 10-1 have an oriented texture which

indicate layering. A part of thin section 10-1 has smaller grains than the rest of the thin section with a mean grain size interval of 100-135 μm.

The sandstones consist of 33-62 % quartz, 7-17 % feldspar and 2-3 % lithic fragments with general size intervals of 125-650 μm, 100-590 μm and 150-1 200 μm respectively. Note that some grains have larger sizes, but these sizes are not abundant.

Undulatory quartz is the most abundant type among the quartz grains. They are subrounded to rounded, elongated and oval with medium to high sphericity and they often have inclusions in them, like zircon. The non-undulatory quartz grains have the same characteristics as the undulatory quartz grains.

The polycrystalline quartz grains have the same characteristics as the monocrystalline quartz grains. 56-74 % of the polycrystalline quartz grains are of metamorphic origin with elongated and undulatory indented crystals with direction and sutured contacts among them, whereas 26-44 % are of plutonic origin, often with mosaic structure with no direction and straight contacts (Appendices 2, 4). Coarse-crystalline chert, or microcrystalline quartz, appear as rounded with high sphericity. They are dirty-looking with black dots in thin section 9-1 and 10-1, but they are not abundant (< 1 %).

The feldspar grains usually lack twinning and the cleavage directions are usually not visible. Plagioclase and alkalifeldspar are approximately equally abundant with thin section 6-1 as an exception, where alkalifeldspar is more abundant than plagioclase. In thin section 10-1, polysynthetic and cross-hatched twins are observed in plagioclase and alkalifeldspar grains respectively, although not commonly. The feldspar grains are often dirty and subrounded with medium sphericity and they have rectangular or tabular shapes. It is common that these grains are partly dissolved and sometimes replaced by carbonate or hematite cement, and in these cases, the grains may have more irregular shapes. Illitization of feldspar is common.

Muscovite appears in all the sandstones except for thin section 6-1, while biotite appear as either green or brown-colored in thin sections 9-1 and 10-1. These phyllosilicate minerals are not abundant (< 3 %). Opaque minerals appear in thin section 10-1 and a small amount of unknown and dark red-colored, dirty-looking grains with undulatory extinction and triangular

shapes appear in both samples. These types of grains result in the unknown grains in thin sections 9-1 and 10-1, but they are also observed in thin section 7-1.

The lithic fragments in the sandstones are usually elongated and subrounded to rounded with medium sphericity and they consist mainly of quartz and feldspar, but may also contain muscovite. Amongst the lithic fragments in the sandstones, the second point counting revealed that 60-74 % of them are of metamorphic origin, whereas 26-35 % are of plutonic origin and 3-5 % are mafic volcanic (Appendices 2, 4). The volcanic clasts were not present in thin section 7-1 and they were only observed in thin section 6-1. The metamorphic and plutonic lithic fragments have the same characteristics as the ones in the conglomerate in thin section 6-7. In addition, other metamorphic lithoclasts are present in the sandstones in thin sections 9-1 and 10-1. Metapelite occurs in both samples, while metapsammite occurs only in thin section 9-1. The metapelite clasts are ductile, elongated and rounded with an abundance of phyllosilicate minerals within the clast with a specific direction. There is also direction in the metapsammite clasts and they consist mostly of quartz, feldspar and muscovite. The mafic volcanic lithic fragments are dirty-looking and dark with high sphericity, small, white crystals and a brown-colored groundmass. Some of the volcanic clasts have needles of plagioclase in the very fine groundmass.

The accessory minerals that are observed are similar for thin sections 7-1 and 9-1, where chert and opaque minerals are observed. In thin section 6-1, biotite, chert and apatite are observed in addition to metapsammite, metapelite and mafic volcanic lithoclasts. These minerals and clasts are not abundant. Illite cement is also observed in thin section 6-1.

The sandstones only have 1-5 % porosity which appear mostly as intergranular pores, but cement occurs more commonly with 15-41 %. The most common cement types are illite, hematite and carbonate cement. The illite cement appear as both needles in the pore space and as rims around the grains. An angle of 70-80° between the cleavage directions has been observed in the carbonate cement, but it is not always visible. Otherwise, quartz, feldspar, kaolinite and illite/sericite cement occur in addition to intergranular cement types (hematite, carbonate and illite), quartz matrix and phyllosilicate matrix. Gypsum cement is observed in thin sections 7-1 and 9-1. During preparation, a lot of grains have fallen out, hence the high amount of voids of 3-13 %.

5. Discussion

From the map of the basement lithologies (Figure 12), it is evident that there is a variation of crystalline basement rocks in the Norwegian North Sea, and an explanation for this may be that the basement material in the area was originally from two different domains (Laurentia and Baltica) that were reworked during the Caledonian Orogeny (Coward, 1995). This may be the reason why there are large variations in the lithologies between and within the three zones in this study.

The different basement lithologies that were observed in this study sometimes are in disagreement with those described by Riber et al. (2015), Bassett (2003) and Slagstad et al. (2011). Bassett (2003) classified the basement rock in well 8/3-1 as a biotite schist which fits with the observations in core 4 and most of core 5, but the macroscopical observations from the deeper parts of core 5 do not confirm such a large content of biotite, hence not a very dark color. However, this may be due to intrusions of granite.

The relatively light-colored basement rock in well 16/1-4 has been classified as a hornblende-gabbro and a leucogabbro in other publications such as Riber et al. (2015) and Slagstad et al. (2011) respectively. Normally, a gabbro is dark-colored, and the presence of hornblende is more common in a diorite than in a gabbro, although it may appear in hornblende-gabbro (Pichler and Schmitt-Riegraf, 1997; Fossen, 2008). Therefore, due to the light color and the content of hornblende, it is more likely to be a diorite than a gabbro.

Monzogranite is observed in wells 16/3-2, 16/4-1 and 16/5-1, but the XRD analysis performed by Riber et al. (2015) often suggests another distribution between plagioclase and alkalifeldspar than observed in this study, resulting in different lithologies. This is the case for wells 16/4-1 and 16/5-1, where the basement rocks are classified as granodiorites in the study of Riber et al. (2015) instead of monzogranites. In some wells, the quartz crystals are not visible macroscopically, although the XRD analysis from Riber et al. (2015) suggests a relatively high amount of the mineral. An example of this is the classified monzodiorite in well 16/1-12, which is referred to as a granodiorite according to Riber et al. (2015).

The red color around the fractures in the greyish areas of the rock in well 16/1-12 may be due to circulation of fluids, but for well 16/5-1 on the other hand, the situation is opposite where

the surrounding areas of several fractures have lost their red color. A possible theory is that the alkalifeldspar crystals around the fractures in well 16/5-1 may have lost their red color as the iron may have been affected, where Fe^{3+} may have been reduced to Fe^{2+} due to circulation of reducing fluids in the fractures, resulting in removal of the red color (Parry et al., 2004). This would leave the surrounding areas relatively colorless, similar to the bleaching process of red sandstones as described by Parry et al. (2004).

One theory that can explain the metasedimentary rock overlying the granite in well 16/4-1 is that the granite may have been succeeded by meta-sediments that have been exposed to high temperatures, resulting in a layered metasedimentary rock (Rutland & Sutherland, 1968). Another possible theory is that the metamorphic rock could have been displaced on top of the granite as a result of faulting, but then the contact would have been relatively sharp instead of the observed succeeding one. The light greenish yellow color in the rock resembles the one of epidote and the content of this mineral in the metasandstone can be explained by possible replacement of carbonate that was initially in the rock (Bird and Spieler, 2004).

Due to the different lithologies in the basement rock in well 16/1-17, different types of clasts can be found in the surrounding areas. Clasts can either be felsic and fresh from the intrusions of granite, or mafic and weathered from the host rock. Mafic material weathers faster than felsic material as mafic minerals tend to be more unstable and less resistant to weathering than felsic minerals, which can be an explanation to why the granite is fresh while the host rock in the basement is severely weathered (Fossen, 2008). This mafic rock has most likely been fractured and exposed on the surface. In this process, material from the surface has most likely filled the fractures, hence the sandstone section observed in the core. The clasts present in the sandstone section are not of basement material, and therefore this is the most reasonable explanation. This will also argue for no tectonic activity in the subsurface. Similarly, the conglomerate surrounding the fractured areas in well 25/11-1 may also be a result of the same process as for the sandstone in well 16/1-17, although clasts from the fresh basement rock are present, indicating that fragments were torn loose during the fracturing of the rock.

The porphyritic texture in the rock in well 16/6-1 does not indicate a dacite as argued for in Riber et al. (2015), but rather an andesite with porphyritic texture, although Riber et al. (2015) also mentioned that it could be on the border between dacite and quartz andesite. Neither the petrographically observations nor the observations from the core viewing identified enough

quartz as porphyroblasts or in the groundmass for this rock to be classified as a dacite or a quartz andesite, which makes it evident that this rock most likely is an andesite. The plutonic section in the end of the core is described as a mica schist by Bassett (2003), but in the thin section provided in this thesis, it looks plutonic and not metamorphic, which argues that the classification in this study is more likely than the one of Bassett (2003). However, the macroscopic observations do not indicate a plutonic origin as it resembles the andesite, only without the porphyroblasts. As a result, clasts in sedimentary rocks in the vicinity that resembles the basement rock can be either volcanic or plutonic in origin. In addition, the observed quartz vein in the core may lead to a high content of monocrystalline quartz in surrounding sedimentary rocks.

There are different opinions on the lithology of the basement rock in well 25/11-1, where Bassett (2003) suggests that it consist of augengneiss, marble and greenschist, whereas Riber et al. (2015) suggests a gneissic schist. Based on the observations in the study, the light colored gneiss may be completely different from the overlying schist-looking rock as it is not deformed or weathered. This means that lithic fragments in sedimentary rocks in the vicinity of the well may either be weathered and resemble a schist, or fresh and resemble light gneiss, implying transport from the same rock type.

The augen in well 35/3-4 can suggest that the rock has a magmatic origin as they most likely are squeezed alkalifeldspar crystals from a former coarse-crystalline rock, such as a granite (Fossen, 2008; Pichler and Schmitt-Riegraf, 1997).

The lithic fragments in the sandstones and conglomerates in this study suggests that both local and underlying basement rocks in the western part of the North Sea can be possible source rocks to the Permian Rotliegend Group in the area. Well 16/1-17 and well 25/10-2R are among the wells that show clasts in the Rotliegend conglomerates that have an abundance of clasts that resemble the underlying basement rock or intrusions in the underlying basement rock. A theory that can explain this is the faulting and reactivation of basement faults in the Early Permian that may have brought clasts of the basement rock up to the surface to be deposited amongst other Rotliegend materials (Leeder and Hardman, 1990). Some of the granitic clasts in the conglomerate in well 16/1-17 are fresher than the others and resemble the granitic intrusions in the basement, while the other granite clasts are more similar to the granites further south on the Utsira High. The conglomerate in well 25/10-2R also show

granitic clasts resembling the granites from sector 16 on the Utsira High in addition to volcanic clasts resembling the andesite in well 16/6-1. These clasts may have had a long transport route considering their subrounded appearance (Pettijohn et al., 1987). According to Berland et al. (2022), the conglomerate in well 16/2-13A also show subrounded granitic clasts that resembles the ones south on the Utsira High. The granite and andesite clasts in these conglomerates may indicate that the granitic basement rocks in sector 16 can be source rocks for Rotliegend material located N-NW from this granitic area and that the main sediment transport direction for the erosive products in the western part of the Norwegian North Sea is towards N-NW (Figure 12). Berland (2022) argues for a sediment transport direction towards NW as the granitic clasts in well 17/4-1 most likely originates from the Sele High, which according to Bartholomew et al. (1993) consist of granite. Lundmark et al. (2013) have also indicated a dominance of sediment influx from the south connected to the Variscan Orogeny, which strengthens the theory in this thesis of a main sediment transport in the N-NW direction in the Permian in the western sector of the Norwegian North Sea.

There are most likely other crystalline rocks that have acted as source rocks for the Rotliegend unit. One example is from well 25/10-2R, where the metamorphic clasts do not resemble the metamorphic gneisses observed in this thesis in the vicinity, which indicate another metamorphic source rock. The abundance of polycrystalline quartz grains and lithic fragments of metamorphic origin in sector 9 and 15 also argues for metamorphic source rocks in the surrounding areas. Thin section 10-1 in well 15/9-9 indicate an abundance of metamorphic polycrystalline clasts, and therefore also a metamorphic source rock nearby. In addition, the petrography from Berland (2022) of thin sections from well 25/10-2R indicate syenite clasts, which argues that a syenite is a source rock to this conglomerate.

The most abundant lithic fragments in the thin sections from the fractured basement rock in well 2/6-5 are the ones resembling the underlying basement rock, which is a phyllite. Similar metamorphic lithic fragments are also observed in sample 6-7 in well 2/7-31, which implements that a metamorphic rock, most likely a phyllite, is a source rock to this area. In contrast to the suggested main transport direction in the west, the direction from well 2/6-5 to well 2/7-31 would be NE-SW (Figure 1). More wells in the area south of well 2/7-31 and in the vicinity of the well would be needed to suggest another transport direction than the one observed in the west as there might be similar lithologies as the phyllite in well 2/6-5 further south as well.

As there are no sedimentary samples from the northern Norwegian sector in this study, it is not possible to indicate possible source rock areas in this part of the North Sea.

6. Conclusion

As a conclusion, this study indicates that both local and underlying basement rocks in the southern and western parts of the Norwegian North Sea may be potential source rocks for the Permian Rotliegend Group in the vicinity due to faulting and erosive processes that affected the pre-Devonian basement in the Early Permian. The western region of the Norwegian sector indicates a main sediment transport direction towards N-NW as lithic fragments resembling basement rocks in the southern part of the Utsira High have been observed in conglomerates towards N-NW. The basement lithology map and the reconstruction of the post-Variscan transport direction in the Norwegian North Sea may help visualize the physical and tectonic processes that affected offshore Norway in the Paleozoic.

7. References

Bartholomew, I. D., Peters, J. M. and Powell, C. M., 1993. Regional structural evolution of the North Sea; oblique slip and the reactivation of basement lineaments. Geological Society, London, Petroleum Geology Conference Series, 4(1), 1109-1122. https://doi.org/10.1144/0041109.

Bassett, M. G., 2003. Sub-Devonian geology. In: Evans, D., Graham, C., Armour, A. and Bathurst, P. (editors), 2003.The Millennium Atlas: petroleum geology of the central and northern North Sea. The Geological Society of London, London, 61-63.

Berland, L. E., 2022. Geomorfologisk effekt på sedimentær sammensetning i den permiske Rotliegend-gruppen i Nordsjøen. Bachelor Thesis, University of Stavanger, 51 pp.

Bird, D. and Spieler, A., 2004. Epidote in geothermal systems. Reviews in Mineralogy and Geochemistry, 56(1), 235-300. https://doi.org/10.2138/gsrmg.56.1.235.

Coward, M. P., 1995. Structural and tectonic setting of the Permo-Triassic basins of northwest Europe. In: Boldy, S. A. R. (editor), 1995. Permian and Triassic Rifting in Northwest Europe, Geological Society Special Publication, 91, 7-39.

Coward, M. P., Dewey, J. F., Hempton, M., Holroyd, J. and Mange, M. A., 2003. Tectonic evolution. In: Evans, D., Graham, C., Armour, A., and Bathurst, P. (editors), 2003.

The Millennium Atlas: petroleum geology for the central and northern North Sea. The Geological Society of London, London, 17-33.

Dickinson, W. R., 1970. Interpreting detrital modes of graywacke and arkose. Journal of Sedimentary Petrology, 40(2), 695-707.

Fossen, H., 2008. Geologi: Stein, mineraler, fossiler og olje. Fagbokforlaget, Bergen, 169 pp.

Fossen, H., Dallman, W. and Andersen, T. B., 2008A. The mountain chain rebounds and founders. In: Ramberg, I. B., Bryhni, L., Nøttvedt, A. and Rangnes, K. (editors), 2008. The Making of a Land – Geology of Norway. Norsk Geologisk Forening, Trondheim, 232-259.

Fossen, H., Pedersen, R., Bergh, S. and Andresen, A., 2008B. Creation of a mountain chain. In: Ramberg, I. B., Bryhni, L., Nøttvedt, A. and Rangnes, K. (editors), 2008. The Making of a Land – Geology of Norway. Norsk Geologisk Forening, Trondheim, 178-231.

Francis, E. H., 1987. Igneous activity in a fractured craton. Carboniferous volcanism in northern Britain. In: Bowes, D. R. and Leake, B. E. (editors), 1987. Crustal evolution in northwest Britain and adjacent regions. Special Publication of the Geological Society of London, 10, 279-296.

Gee, D. G., Janák, M., Majka, J., Robinson, P. and Van Roermund, H., 2012. Subduction along and within the Baltoscandian margin during closing of the Iapetus Ocean and Baltica-Laurentia Collision. Lithosphere, 5(2), 169-178. doi: 10.1130/L220.1.

Glennie, K. W., 1990A. Lower Permian – Rotliegend. In: Glennie, K. W. (editor), 1990. Introduction to the petroleum geology of the North Sea, 3rd ed. Blackwell Scientific Publications, Oxford, 120-152.

Glennie, K. W., 1990B. Outline of North Sea history and structural framework. In: Glennie, K. W. (editor), 1990. Introduction to the petroleum geology of the North Sea, 3rd ed. Blackwell Scientific Publications, Oxford, 34-77.

Ingersoll, R. V., Bullard, T. R., Ford, R. L., Grimm, J. P., Pickle, J. D. and Sares, S.W., 1984. The effect of grain size on detrital modes: A test of the Gazzi-Dickinson point-counting method. Journal of Sedimentary Petrology, 54, 103-116.

Larsen, B. T., Olaussen, S., Sundvoll, B. and Heeremans, M., 2008. Volcanoes and faulting in an arid climate. In: Ramberg, I. B., Bryhni, L., Nøttvedt, A. and Rangnes, K. (editors), 2008. The Making of a Land – Geology of Norway. Norsk Geologisk Forening, Trondheim, 260-303.

Leeder, M. R. and Hardman, M., 1990. Carboniferous geology of the southern North Sea and controls on hydrocarbon prospectivity. In: Hardman, R. F. P. and Brooks, J. (editors), 1990. Tectonic Events Responsible for Britains Oil and Gas reserves. Special Publication of the Geological Society of London, 55, 87-105.

Longiaru, S., 1987. Visual Comparators for Estimating the Degree of Sorting from Plane and Thin Section. Journal of Sedimentary Petrology, 57, 791-194.

Lundmark, A. M., Bue, E. P., Gabrielsen, R. H., Flaat, K., Strand, T. and Ohm, S. E., 2013. Provenance of late Palaeozoic terrestrial sediments on the northern flank of the Mid North Sea High: detrital zircon geochronology and rutile geochemical constraints. Geological Society of London Special Publications, 386, 243-259. doi: 10.1144/SP386.4.

McKerrow, W., Mac Niocaill, C. and Dewey, J., 2000. The Caledonian Orogeny redefined. Journal of the Geological Society, 157(6), 1149-1154.

Nichols, G., 2009. Sedimentology and Stratigraphy, 2nd ed. Wiley-Blackwell, Chichester, England, 419 pp.

NPD, 2021A. https://factpages.npd.no/nb-no (visited 27/12-21).

NPD, 2021B. https://factpages.npd.no/nb-no/strat/pageview/litho/groups/10 (visited: 27/12-21).

NPD, 2022. https://factmaps.npd.no/factmaps/3_0/ (visited: 01/05-22).

Olesen, O., Ebbing, J., Gellein, J., Kihle, O., Myklebust, R., Sand, M., Skilbrei, J. R., Solheim, D. and Usov, S., 2010. Gravity anomaly map, Norway and adjacent areas. Scale 1:3 million. Geological Survey of Norway.

Osagiede, E., Rotevatn, A., Gawthorpe, R., Kristensen, T., Jackson, C. and Marsh, N., 2020. Pre-existing intra-basement shear zones influence growth and geometry of non-colinear normal faults, western Utsira High-Heimdal Terrace, North Sea. Journal of Structural Geology, 130, 18 pp. https://doi.org/10.1016/j.jsg.2019.103908.

Parry, W., Chan, M. and Beitler, B., 2004. Chemical bleaching indicates episodes of fluid flow in deformation bands in sandstone. AAPG Bulletin, 88(2), 175-191. https://doi.org/10.1306/09090303034.

Pichler, H. and Schmitt-Riegraf, C., 1997. Rock-forming minerals in thin section, 2nd ed. Chapman & Hall, 220 pp.

Pettijohn, F. J., Potter, P. E. and Siever, R., 1987. Sand and Sandstone, 2nd ed. Springer-Verlag, New York, 340 pp.

Riber, L., Dypvik, H. and Sørlie, R., 2015. Altered basement rocks on the Utsira High and its surroundings, Norwegian North Sea. Norwegian Journal of Geology, Oslo, 95(1), 57-89. http://dx.doi.org/10.17850/njg95-1-04.

Rutland, R. W. R. and Sutherland, D. S., 1968. The chemical composition of granitic gneisses and spragamitic meta-sediments in the Glomfjord region, Northern Norway. Norsk geologisk tidsskrift, 48, 365-380.

Slagstad, T., Davidsen, B. and Daly, J. S., 2011. Age and composition of crystalline basement rocks on the Norwegian continental margin; offshore extension and continuity of the Caledonian – Appalachian orogenic belt. Journal of the Geological Society, London, 168, 1167-1185. https://doi-org.ezproxy.uis.no/10.1144/0016-76492010-136.

Wentworth, C. K., 1922. A Scale of Grade and Class Terms for Clastic Sediments. The Journal of Geology, 30, 377-392.

Wiest, J., Jacobs, J., Fossen, H., Ganerod, M. and Osmundsen, P., 2020. Segmentation of the Caledonian orogenic infrastructure and exhumation of the Western Gneiss region during transtensional collapse. Journal of the Geological Society, 178(3). https://doi-org.exproxy.uis.no/10.1144/jgs2020-199.

Worsley, D. and Nøttvedt, A., 2008. Vast lowland plains, coal and salt. In: Ramberg, I. B., Bryhni, L., Nøttvedt, A. and Rangnes, K. (editors), 2008. The Making of a Land – Geology of Norway. Norsk Geologisk Forening, Trondheim, 304-329.

Ziegler, P. and Shell International Petroleum Company, 1982. Geological atlas of Western and Central Europe. The Hague: Shell Internationale Petroleum Maatschappij B.V., 130 pp.

8. Appendix

8.1. Appendix 1: Classification of sandstones and conglomerates after McBride (1963)
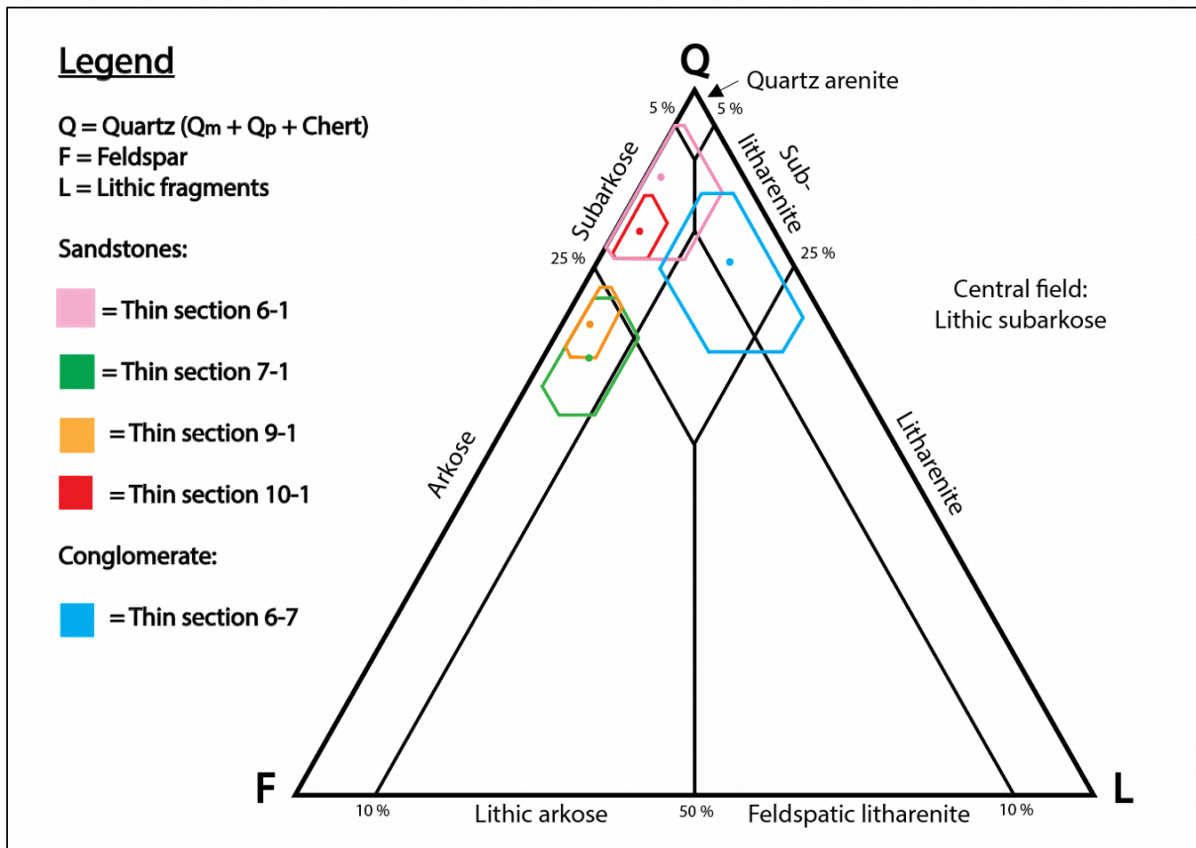
8.2.Appendix 2: Triangle diagram for lithic fragments
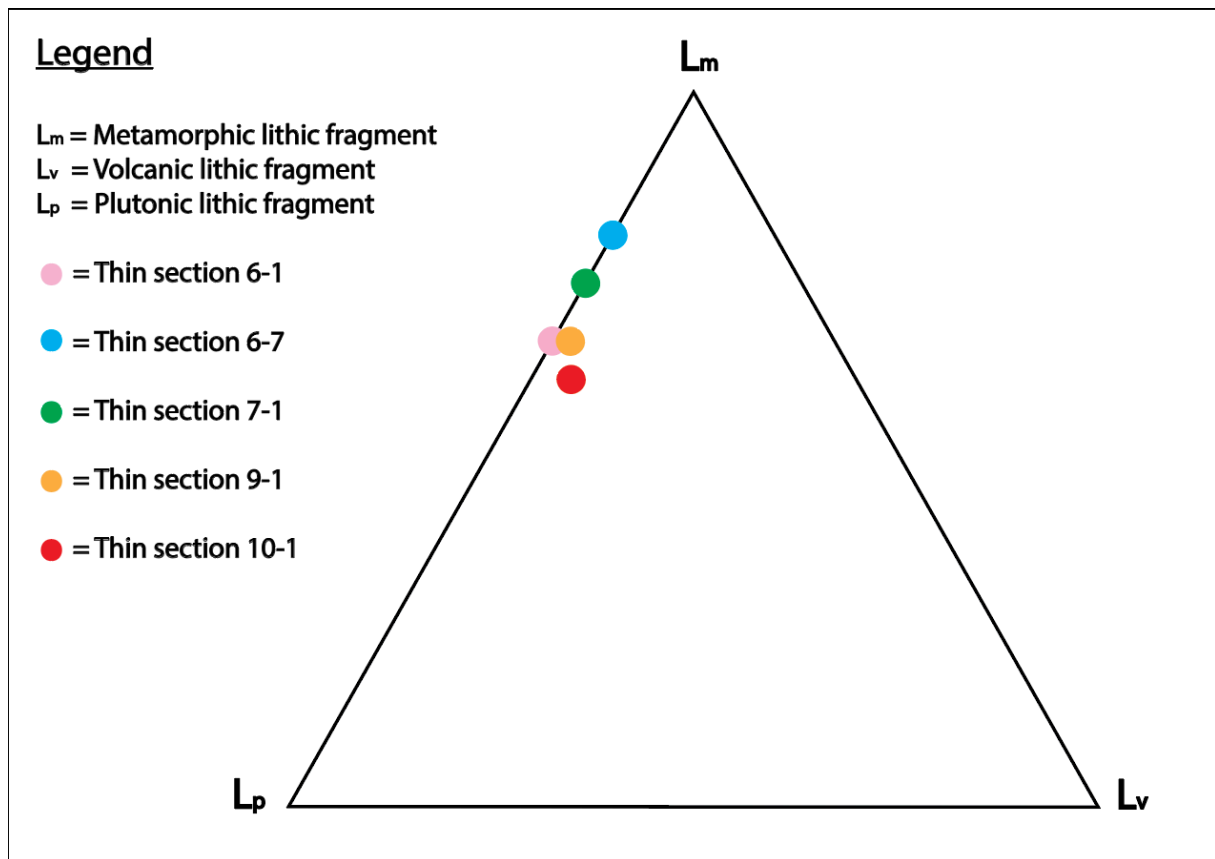
8.3. Appendix 3: Thin section protocol – All components

	6-1		6-7		7-1		9-1		10-1	
	Count	%	Count	%	Count	%	Count	%	Count	%
Detrital components & lithoclasts										
$Q_{m,\ undulatory}$	21	30.9	15	20.3	45	17.0	127	18.8	151	22.0
$Q_{m,\ non\text{-}undulatory}$	8	11.8	10	13.5	21	8.0	83	12.3	81	11.8
$Q_{polycrystalline}$	13	19.1	14	18.9	21	8.0	8	1.2	24	3.5
Chert	–	–	2	2.7	–	–	2	0.3	2	0.3
Total Q	**42**	**61.8**	**41**	**55.4**	**87**	**33.0**	**220**	**32.6**	**258**	**37.6**
Plagioclase	1	1.5	–	–	8	3.0	9	1.3	8	1.2
Alkalifeldspar	4	5.9	–	–	–	–	8	1.2	18	2.6
Feldspar (not defined further)[1]	–	–	4	5.4	21	8.0	34	5.0	17	2.5
Dissolved feldspar (not specified further)	–	–	–	–	16	6.1	42	6.2	12	1.7
Dissolved Alkalifeldspar	–	–	–	–	–	–	5	0.7	1	0.1
Sum F	**5**	**7.4**	**4**	**5.4**	**45**	**17.0**	**98**	**14.5**	**56**	**8.2**
Muscovite	**–**	**–**	**–**	**–**	**1**	**0.4**	**9**	**1.3**	**15**	**2.2**
Biotite	**–**	**–**	**–**	**–**	**–**	**–**	**1**	**0.1**	**2**	**0.3**
Opaque minerals	**–**	**–**	**–**	**–**	**–**	**–**	**–**	**–**	**5**	**0.7**
Sum L	**1**	**1.5**	**9**	**12.2**	**8**	**3.0**	**11**	**1.6**	**10**	**1.5**
Unknown grain[2]	**–**	**–**	**–**	**–**	**–**	**–**	**4**	**0.6**	**1**	**0.1**
Total grains/percentage	**48**	**70.6**	**54**	**73.0**	**141**	**53.4**	**343**	**50.8**	**347**	**50.6**
Porosity & Cement										
Intergranular porosity	1	1.5	5	6.8	14	5.3	17	2.5	9	1.3
Intragranular porosity	–	–	–	–	–	–	6	0.9	–	–
Total porosity	**1**	**1.5**	**5**	**6.8**	**14**	**5.3**	**23**	**3.4**	**9**	**1.3**
Quartz cement	4	5.9	1	1.4	6	2.3	7	1.0	5	0.7

Feldspar cement	1	1.5	–	–	–	–	3	0.4	2	0.3
Hematite cement	5	7.4	–	–	41	15.5	71	10.5	84	12.2
Intragranular hematite cement	–	–	–	–	–	–	17	2.5	9	1.3
Carbonate cement	–	–	–	–	19	7.2	119	17.6	132	19.2
Intragranular carbonate cement	–	–	–	–	–	–	16	2.4	8	1.2
Illite cement	–	–	4	5.4	20	7.6	29	4.3	–	–
Intragranular illite cement		–	–	–	–	–	2	0.3	–	–
Illite/Sericite cement	–	–	–	–	–	–	8	1.2	–	–
Kaolinite	–	–	–	–	–	–	3	0.4	30	4.4
Total Cement	**10**	**14.7**	**5**	**6.8**	**86**	**32.6**	**275**	**40.7**	**270**	**39.3**
Quartz matrix	–	–	–	–	12	4.5	8	1.2	–	–
Phyllosilicate matrix	–	–	10	13.5	4	1.5	4	0.6	–	–
Total Matrix	**–**	**–**	**10**	**13.5**	**16**	**6.1**	**12**	**1.8**	**–**	**–**
Void – grain has fallen out	**9**	**13.2**	**–**	**–**	**7**	**2.7**	**22**	**3.3**	**61**	**8.9**
Total	**68**	**100.1**	**74**	**100.1**	**264**	**100.1**	**675**	**99.9**	**687**	**100.1**

[1]The feldspar grains that are not classified further do not show characteristics like cleavage directions and twinning.

[2]The unknown grains are dark red-colored and dirty-looking with triangular shapes and undulatory extinction.

8.4. Appendix 4: Thin section protocol – Polycrystalline grains

	6-1		6-7		7-1		9-1		10-1	
	Count	%	Count	%	Count	%	Count	%	Count	%
$P_{Q, m}$	9	28	11	50	35	43	27	31	15	29
$P_{Q, p}$	6	19	6	27	12	15	10	11	12	23
Sum P_Q	**15**	**47**	**17**	**77**	**47**	**58**	**37**	**43**	**27**	**52**
L_m	11	34	4	18	23	28	20	23	11	21
Metapelite	–	–	–	–	–	–	4	5	1	2
Metapsammite	–	–	–	–	–	–	2	2	–	–
L_p	6	19	1	5	8	10	13	15	7	13
$L_{v, maf}$	–	–	–	–	–	–	1	1	1	2
Sum L	**17**	**53**	**5**	**23**	**31**	**38**	**40**	**46**	**20**	**38**
Chert	**–**	**–**	**–**	**–**	**3**	**4**	**10**	**11**	**5**	**10**
Sum	**32**	**100**	**22**	**100**	**81**	**100**	**87**	**100**	**52**	**100**

P_Q = Polycrystalline quartz, $P_{Q,m}$ = Metamorphic polycrystalline quartz, $P_{Q,p}$ = Plutonic polycrystalline quartz, L = Lithic fragments (Lithoclasts), L_m = Metamorphic lithic fragment, L_p = Plutonic lithic fragment, $L_{v, maf}$ = Mafic volcanic lithic fragment.